https://doi.org/10.1016/j.energy.2017.12.020

Title: Development and experimental study of a novel plate dehumidifier made of anodized aluminum

Author: Tao Wen[1], Lin Lu[1, *], Chuanshuai Dong[1] , Yimo Luo[2]

[1]Renewable Energy Research Group, Department of Building Services Engineering, The Hong Kong Polytechnic University, Hong Kong, China

[2]Faculty of Science and Technology, Technological and Higher Education Institute of Hong Kong, Hong Kong, China

Abstract: The falling film dehumidifier is a key component in the liquid desiccant cooling system (LDCS). However, the most commonly used metals, such as steel and aluminum, can hardly resist the erosion of liquid desiccant. It greatly limits the fabrication of compact dehumidifiers and hinders the promotion of LDCS. The present study introduced a novel falling film dehumidifier which was made by the metal of anodized aluminum. Experiments were carried out to compare the dehumidification performance between ordinary aluminum dehumidifier and anodized one. The influences of air temperature, mass flow rate, inlet humidity and solution temperature, mass flow rate, temperature on dehumidification performance were identified. The results showed that the anodized aluminum could alleviate the erosion significantly. In addition, with the surface treatment by anodizing, the contact angle of lithium chloride solution decreased from 85.2^{o} on an ordinary aluminum plate to 43.1^{o} on an anodized one. Accordingly, the wetting area on the plate dehumidifier increased from 0.143m^2 to 0.178m^2 with a 24.5% increment at certain operating conditions. Both the absolute moisture removal and dehumidification effectiveness increased in various degrees for anodized dehumidifier compared with the ordinary type. The relative increments could reach up to 50.6% and 36.7% under certain conditions respectively. The newly introduced anodized aluminum dehumidifiers can not only alleviate the plate corrosion but also improve the dehumidification capability due to smaller surface contact angles, which can be promisingly applied in LDCS.

Key words: liquid desiccant, dehumidifier, falling film, internally cooled, anodized aluminum

Nomenclature			
d	Absolute humidity(g / kg)	ξ	Dehumidification effectiveness (Dimensionless)
G	Flow rate(kg / s)	Δ	Change value
h	Enthalpy(kJ / kg)	Subscripts	
$LDCS$	Liquid desiccant cooling system	a	Air
T	Temperature(^oC)	dry	Dry bulb
X	Concentration($\%$)	e	Equilibrium
		in	Inlet
Greek symbols		out	Outlet
φ	Relative humidity($\%$)	s	Solution
ρ	Density(kg / m^3)	w	Cooling water

1 Introduction

The traditional vapor compression cooling system (VCS) has been criticized for its reliance on electricity consumption and limited control ability of dehumidification. Compared with the VCS, the liquid desiccant cooling system (LDCS) is more efficient by handling the sensible and latent load separately. With the quest of high quality life among people in nowadays, the LDCS has shown its unique attraction with the ability to create a more comfortable indoor environment. What is more, the regenerator as another key component in LDCS can make use of low grade energy, such as solar energy, waste heat, during the regeneration of liquid desiccant. Therefore, LDCS is considered as a promising candidate in the cooling field, especially in humid regions, such as Hong Kong.

The existing study focuses on the dehumidification performance of dehumidifier which is one of the main components in LDCS [1-5]. Generally, most dehumidifiers can be classified into three types, i.e. packed bed, falling film dehumidifiers and indirect contact type [1, 2, 4, 6-8]. In a packed bed dehumidifier, the concentrated liquid desiccant is sprayed in the bed and flows along the packed material. The processed air also flows through the space in the bed and contacts with the solution. Due to the partial pressure difference of water vapor between liquid desiccant and air, water vapor in the air is absorbed by the concentrated solution. During this process, latent heat due to water vapor absorption would release. So the solution temperature will increase continually along the flow direction, and this inevitably deteriorates the absorption performance to some degree. In addition, other problems, such as low wetting ability of packed materials, possibility of liquid entrainment, high pressure drop of air, further limit its wide application [2, 4, 5].

In order to solve the problems mentioned above, researchers introduced another kind of absorber, namely falling film absorber. Compared with the packed bed one, the solution can be internally cooled by other media, and it also overcomes liquid entrainment and high pressure loss to a great extent [2, 4, 5]. Researchers have carried out studies to investigate the simultaneous heat and mass transfer characteristics in an internally cooled dehumidifier both numerically and experimentally [1-5]. To summarize, the mathematic models for dehumidifier can be divided into two categories, i.e. effectiveness-NTU model and finite difference model [9]. Their applications can be found for parallel flow, counter flow and cross flow [10-13]. However, in the mathematics model, the properties of materials, such as resistance and corrosion, were not considered and validated.

For tube absorber, Jeong et al. [14] developed a model to predict the heat and mass transfer in falling film and droplet mode flow of a tube absorber. In their model, incomplete wetting was considered by introducing a wetting ratio. After model validation, they studied the effects of different parameters on the dehumidification performance. Three copper tubes with different outer diameters were employed by Yoon et al. [15] to explore the heat and mass transfer characteristics during absorption process. The absorber with smaller diameters showed better heat and mass transfer performance. Luo et al. [16] experimentally studied the performance of a fin-tube internally-cooled dehumidifier and reported a good absorption performance of the fin-tube absorber. In their study, in order to enhance the corrosion resistance performance of the dehumidifier, the surface treatment technology of electroplating was employed. Some antiseptic materials were adhered to the surface of the fin through electroplating. Comparative corrosion resistance tests demonstrated good anti-corrosion performance of the adopted fin-tube dehumidifier and the poor anti-corrosion performance of stainless steel 304 and copper.

However, the dehumidifier based on tubes has lower efficiency and bigger volume compared with the absorbers made by plates [17, 18]. So, the plate type dehumidifier has drawn more attention naturally [14-21]. The dehumidification performance of a stainless steel dehumidifier was studied by Luo et al. [19, 20]. The influence of various parameters which included the film thickness on absorption behavior was identified. Yin et al. [21] studied both the dehumidification and regeneration performance of an internally cooling/heating absorber made by stainless steel. Their results revealed that the heat and mass transfer efficiency of internally-cooled/heated dehumidifier/ regenerator was higher than those adiabatic ones. Gao et al. [22] also conducted experiments to compare the dehumidification effectiveness and moisture removal rate between an internally cooled and an adiabatic dehumidifier. Internally cooled dehumidifier was verified to have higher dehumidification effectiveness and bigger moisture removal rate. However, they did not give detailed information about the dehumidifier. In the work done by Zhang et al. [23], the dehumidifier made of stainless steel was designed and investigated both by experiments and simulation analysis. After the experimental and numerical study of absorption performance under various operating conditions, an internally cooled/heated LDCS system driven by exhaust heat of heat pump was proposed with relatively high COP. In consideration of the strong corrosion of liquid desiccant, Liu et al. [24] introduced an internally-cooling dehumidifier made of thermally conductive plastic. Unlike the normal plastic, the thermal conductivity of the mentioned thermally conductive plastic reaches as high as 16.5 W/(m·K). On one hand, the new dehumidifier could achieve superior corrosion resistance capacity. On the other hand, it had considerable heat and mass transfer performance compared with dehumidifiers made of metals as well. Lee et al. [25] also introduced a kind of plastic dehumidifer made of heat-resistant acrylonitrile butadiene styrene plastic. In order to overcome the low wettability of plastic, hydrophilic coating and groove shape were treated on the surface of the plate. The *Sh* and *Nu* correlations for the process of heat and mass transfer were developed with an error within ±25% according to their experimental results. Mortazavi et al. [18] designed an internally cooled dehumidifier with offset fins made of copper. The new surface sturcture could not only increase the wetting area but also enhance the absorption rate significantly, which made it to be a very promising framework for the development of highly compact absorber.

It is well known that commonly used materials for falling film dehumifier are metals, such as stainless steel [19-21] and copper [18]. But if no special treentment is provided, the plate corrosion would probably occur [16]. Therefore, some surface treatment process, such as electroplating [16], was introduced. Besides, some researchers gave up metal directly and chose special plastic for utilization [24, 25]. However, compared with metals, plastic has the inherent disadvantage of relative low wettability and thermal conductivity. It is quite necessary to find other material alternatives with the excellent anti-corrosion performance, good wettability, high heat conductivity and good workability.

Based on the above observations, the present study newly introduced an anodized aluminum plate for dehumidifiers which has been widely used in heat exchanger. Two single channel aluminum plate dehumidifiers with and without anodizing with the size of 500mm*500mm (Length*Width) were fabricated. The corrosion resistance performance was examined within a period of 30 days. The wettability were identified and compared by the means of contact angles and wetting areas between these two aluminum plates. Finally, the dehumidification performance under various operating conditions was investigated.

2 Research method

2.1 Description of test rig

A test rig was designed and fabricated for the purpose of experimental investigation on the absorption performance of the falling film dehumidifier. The systematical diagram of the test rig was shown in Fig. 1. The system had three loops, i.e. desiccant solution loop, air loop and cooling water loop. Neoprene foam was wrapped on the surface of pipes and channels to insulate the loops from external environment.

Lithium chloride (LiCl) was adopted in the liquid desiccant loop and stored in the tank. A heater installed in the tank could regulate the temperature of the solution. With the assistance of a pump, the solution cycled in the loop and flowed through a by-pass valve firstly. By adjusting the opening of this value, the flow rate of solution in the cycle could be changed. The exact value of flow rate was measured by a turbine flow rate sensor. Once the solution reached the distributor, it spilt through the crack of the distributor and flowed on the surface of the plate dehumidifier in the form of falling film. By contacting with the processed air, liquid desiccant absorbed the water vapor from it under the driven force of the partial pressure difference of water vapor. Then, the solution was collected by a collector and flowed back to a tank. Both the inlet and outlet temperatures of solution were measured by Pt-100 thermocouples. The concentration was not acquired directly but calculated by measuring the temperature and density of the liquid desiccant with a thermocouple and a specific gravity hydrometer respectively. Then, the conversion was achieved via the equation provided by the literature [26]. For the air loop, the air was pumped to the channel by a fan. The flow rate of air could be regulated by a damper. The air humidity was adjusted to the required value by regulating the input power of an electric humidifier. The air temperature was controlled by an electric heater with an automatic Proportion-Integration-Differentiation (PID) controller. The input humidification amount of the electric humidifier was regulated by adjusting the input voltage signal ranging from 1 to 10V. Before and after the contact with liquid desiccant, the dry bulb temperatures and relative humidity were measured by the thermocouples and humidity sensors. In addition, at the outlet of the air channel, a Pitot tube which connected with a micro-manometer produced by TSI Company was installed for the purpose of air flow rate measurement. Internal cooling was introduced in the system. Water was cooled by a chiller before pumping into the internally cooling unit. After the heat exchange with solution, water flowed back to tank for next cycle. Both the inlet and outlet temperatures of cooling water were obtained by Pt100 thermocouples. The flow rate of water was acquired by a turbine flow rate sensor. All the data of temperatures, humidity and flow rates were displayed and recorded by a data logger.

2.2 Dehumidification performance indices

Several criteria have been used to evaluate the performance of dehumidification [11-21]. In the present study, two indices, namely absolute moisture removal and dehumidification effectiveness, were chosen to identify the water vapor absorption performance in the single channel absorber. Their definitions are shown in the following part.

Absolute moisture removal (Δd) is defined as [19],

$$\Delta d = d_{a,in} - d_{a,out} \tag{1}$$

where $d_{a,in}$ and $d_{a,out}$ represent the inlet and outlet absolute humidity respectively. This index can indicate the absolute humidity change before and after absorption process directly. As a result, it is often employed by researchers when the outlet humidity content is the main concern.

The absolute air humidity was not measured directly but by the conversion via the measured dry bulb temperature and relative humidity. Their relationship can be described as follows [27]:

$$ln(p_{w,s}) = \frac{c_1}{T_{dry}} + c_2 + c_3 T_{dry} + c_4 T_{dry}^{\ 2} + c_5 T_{dry}^{\ 3} + c_6 T_{dry}^{\ 4} + c_7 ln(T_{dry}) \quad (2)$$

$$d = 0.622 * \frac{\varphi p_{w,s}}{101325 - \varphi p_{w,s}} \quad (3)$$

where T_{dry} is the air dry bulb temperature and φ is the relative humidity. The constants in Equation 2 are:

$$c_1 = -5800.2206,\ \ c_2 = 1.3914993,\ \ c_3 = -0.048640239$$
$$c_4 = 0.41764768 \times 10^{-4}, c_5 = -0.14452093 \times 10^{-7}, c_7 = 6.5459673$$

Dehumidification effectiveness (ξ) is defined as [22, 24],

$$\xi = \frac{d_{a,in} - d_{a,out}}{d_{a,in} - d_{e,in}} \quad (4)$$

In equation 4, $d_{e,in}$ is the absolute moisture content of the processing air in the condition of equilibrium with inlet desiccant solution at its concentration and temperature. It is worth mentioning that in present study the flow pattern between processed air and solution is countercurrent. The minimum absolute moisture content of outlet air is the equivalent moisture content of inlet solution at its temperature and concentration. Therefore, the maximum dehumidification effectiveness is 1. However, when the flow pattern is parallel, the dehumidification effectiveness may be greater than 1 at high solution inlet temperature and low cooling water temperature. Under such circumstance, the inlet solution temperature should be replaced by inlet cooling water temperature when calculating the equivalent moisture content [12, 24]. This criterion indicates the ratio of actual moisture removal amount to potential greatest moisture removal and shows the efficiency of a dehumidifier. It has the same meaning with heat transfer efficiency for a heat exchanger.

2.3 Uncertainty analysis and experimental validation

During the experiments, working conditions were changed by regulating the corresponding actuators. The detailed operating conditions are summarized and specified in Table 1. Generally speaking, all experimental parameters during the data processing can be classified into two groups, i.e. the directly measured group and indirectly measured group. They are judged by whether they can be measured by sensors directly or not. The uncertainties of the former group are obtained according to the accuracies of sensors, and the later ones are calculated based on the method of uncertainty propagation which is shown in Equation 5 [28]. The uncertainties for all parameters are summarized and listed in Table 2.

$$\frac{\delta y}{y}=\sqrt{(\frac{\partial \ln f}{\partial x_1}\delta x_1)^2+(\frac{\partial \ln f}{\partial x_2}\delta x_2)^2+...+(\frac{\partial \ln f}{\partial x_n}\delta x_n)^2} \quad (5)$$

where y indicates the indirect measured parameter and δx_n represents the uncertainty of the n_{th} direct measured parameter. The relationship between y and x_i can be described by Equation (5).

$$y=f(x_1,x_2,...,x_i,...,x_n) \quad (6)$$

Simultaneous heat and mass transfer took place in the single channel dehumidifier where water vapor absorption occurs. During this process, both the energy and mass conservation equations must be satisfied. The equations can be expressed as follows:

$$G_s(h_{s,o}-h_{s,i})=G_a(h_{a,i}-h_{a,o})+G_w(h_{w,i}-h_{w,o}) \quad (7)$$

$$G_a(d_{a,i}-d_{a,o})=G_sX_{s,i}(\frac{1}{X_{s,o}}-\frac{1}{X_{s,i}}) \quad (8)$$

In equation 7, G_s and G_a represents the mass flow rate of solution and air respectively. h stands for enthalpy. The subscripts s, a, w indicate the solution, air and cooling water correspondingly. The inlet and outlet parameters are differentiated by the other letter i, o in the subscript.

During the dehumidification experiments, the absolute humidity changes were found to be less than 5g/kg in all conditions. Although the change of air humidity could be detected by humidity sensor, the concentration change of liquid desiccant was too small to be measured accurately in one cycle. So, only the energy conservation equation was validated in the present study. As shown in Fig. 2, most of the validation data fall into the error band of $\pm 15\%$. Therefore, the rationality of the test rig can be proved adequately.

3 Results and discussion

3.1 The corrosion resistance performance

To enhance the corrosion resistance ability of ordinary aluminum plate, the widely used surface treatment technology of anodizing was firstly employed for dehumidifier plates. During the anodizing, the aluminum plate was inserted into an acid bath, and oxidized by electrochemical reactions. After that, a dense aluminum oxide layer was formed on the surface of ordinary aluminum [29]. As a result of the protection by such an aluminum oxide film, the erosion of plates can be greatly resisted. Two aluminum plates with and without anodizing were immersed in the lithium chloride solution with the concentration of 38% at room temperature for 30 days to test the corrosion resistance performance. Fig. 3 shows the results before and after the corrosion experiment. The rusty spots on the surface of the ordinary aluminum plate can be observed obviously after the test. However, on the surface of the anodized aluminum plate, no such phenomenon was detected. In addition, during the subsequent experimental study, anodized aluminum plate also showed excellent corrosion resistance performance, which proves that the material introduced by present study is suitable for manufacturing dehumidifiers.

3.2 Influence of solution flow rate

The effect of solution flow rate on absorption characteristics are presented in Fig. 4. It is found neither the absolute moisture removal nor the dehumidification effectiveness changes too much with the increase of flow rate. This trend is very different from those of other researchers [19, 24]. During the experiments, it was found that the wetting area almost kept the same even when the solution flow rate increased. The measured values were 0.143m^2 for normal anlumimum dehumidifier and 0.178m^2 for anodized one with the fluctuation less than 0.03m^2. It meant that the film thickness of falling film must increase with the increase of solution flow rate. The increase of solution flow rate enhanced the heat transfer coefficient between cooling wall and solution, which improved the absorption rate subsequently. However, the increase of the film thickness increased the heat transfer resistance and offset this growing tendency. So, the performance of dehumidification showed little relationship with the solution flow rate. On the other hand, the performance difference between ordinary and anodized aluminum plates can be easily observed from Fig. 4. When the flow rate was around 0.1kg/s, the enhancements were found to be as high as 1g/kg and 6.4% for absolute moisture removal and dehumidification effectiveness respectively. The relative average increments were observed to be 45.3% and 36.0% respectively.

3.3 Influence of solution temperature

Fig. 5 shows the influence of inlet solution temperature on dehumidification characteristics. Both the absolute moisture removal and dehumidification effectiveness reduced with the increasing of temperature. Taking the absolute moisture removal for example, when the solution temperature decreases from 34°C to 27°C, the value has a reduction of 0.51g/kg from 2.21g/kg to 1.7g/kg for normal dehumidifier and 1.05g/kg from 2.86g/kg to 1.81g/kg for the other one severally. This trend can be easily explained by the fact that the increase of solution temperature would result in the rise of equilibrium surface vapor pressure on the surface of solution. For the solution concentration of 38%, the equilibrium surface vapor pressure is 808Pa at temperature of 27°C and 1249Pa at temperature of 34°C. Therefore, the driving force for absorption reduced when the humidity of air kept constant. The merit of absorption by adopting anodizing plate was also proved, as shown in Fig. 5. The lower solution temperature was likely to have higher increment, and this could be caused by the higher water vapor difference between solution and air at lower solution temperature.

3.4 Influence of solution concentration

The dehumidification performances of the single channel dehumidifier under three levels of concentrations, namely 35%, 37% and 38%, were investigated. The results are summarized in Fig. 6. It is obvious that higher concentration solution has better dehumidification performance at solution flow rate of 0.1kg/s, because higher concentration means lower equilibrium surface vapor pressure on the surface of solution. The lower vapor pressure results in bigger mass transfer driving force and greater absolute moisture removal subsequently. For the dehumidification effectiveness, even though the increase of concentration enlarges the denominator of it, the increment of numerator is larger and this leads to the rise of dehumidification effectiveness finally. For these three concentrations, the relative enhancements for absolute moisture removal and dehumidification effectiveness were 28.1% and 29.8% averagely.

3.5 Influence of air flow rate

As shown in Fig. 7, the influence of air flow rate on dehumidification ability is illustrated. There is a descending trend for both the absolute moisture change and dehumidification effectiveness with the ascending of air flow rate. The explanation is that the air velocity also increases with the increase of air flow rate. Higher velocity means shorter contact time between air and solution. Even when the mass transfer coefficient is greater at higher velocity [24], the shorter contact time makes both the absolute moisture removal and dehumidification effectiveness smaller. However, the dehumidification rate, defined by the product of absolute moisture removal and air mass flow rate, has an increment corresponding to a rise in air flow rate. When the air flow rate increases from 0.021kg/s to 0.058kg/s, the dehumidification rate also has a distinct increment of 0.048g/s from 0.062g/s to 0.11g/s for the anodized plate. This is caused by the higher mass transfer coefficient under bigger mass flow rate [24]. The mass transfer coefficient increased from 0.0577kg/($m^2\cdot s$) to 0.0775 kg/($m^2\cdot s$) for normal dehumidifier when the air flow rate increased from 0.021kg/s to 0.058kg/s.

3.6 Influence of air dry bulb temperature

The dehumidification characteristics under different temperatures ranging from 28^{o}C to 36^{o}C were identified as shown in Fig. 8. No distinct trend can be concluded for both kinds of dehumidifiers. Both the absolute moisture removal and dehumidification effectiveness fluctuate around certain values when the air temperature changes. Under the operating conditions in this study, the change of air temperature did not change the mass transfer coefficient much, and the change of air temperature did not have a direct influence on the mass transfer force of equilibrium surface vapor pressure difference. However, distinct enhancement for absorption performance is presented in Fig. 8. Averagely speaking, the absolute moisture removal has an increment of 0.51g/kg from 2.49g/kg for aluminum plate to 3.0g/kg for anodized one, and the dehumidification effectiveness increases from 13.5% to 16.3% correspondingly in the temperature from 28^{o}C to 36^{o}C.

3.7 Influence of air inlet humidity

Fig. 9 compares the absorption performance of two dehumidifiers under various inlet air humidity ranging from 17g/kg to 25g/kg. As shown, both the absolute moisture removal and dehumidification effectiveness rise with the growth of inlet humidity. For the absolute moisture removal, when the moisture content of air increases from 17.2g/kg to 24.3g/kg, it changes from 1g/kg to 2.58g/kg for normal plate and 1.35g/kg to 3.33g/kg for anodized one. The dehumidification effectiveness increases from 9.35% to 14.5% for normal one and 11.7% to 18.8% for the other dehumidifier. This can be easily understood as the mass transfer force would increase with the increase of inlet humidity. In addition, the increase of absolute moisture removal on the numerator of dehumidification effectiveness is bigger than the difference between equilibrium humidity and inlet air humidity on the denominator. It causes the increment of dehumidification effectiveness as shown in Fig. 9. The enhancement of dehumidification performance by the employment of anodized aluminum can also be obviously demonstrated in this figure.

3.8 Discussion on dehumidification performance

As shown from Fig. 4 to Fig. 9, the distinct enhancement of dehumidification performance by adopting anodized dehumidfier can be easily concluded. Under various operating conditions, the degrees of improvement are different. When the solution concentration is 35% in Fig. 6, the relative enhancement for absolute moisture removal and dehumidification effectiveness are as high as 50.6% and 36.7% respectively. The main reason can be intuitively contributed to the significant increase of wetting area as shown in Fig. 10. As formulated by Equation 1, the absolute moisture removal is the difference between the inlet and outlet absolute humidity. The outlet absolute humidity is directly determined by the wetting area and mass tranfer coefficient at certain working conditions. When the mass transfer coefficient is the same, the absolute moisture removal is closely related with the wettting area of the dehumidifier. Bigger wetting area directly contributes to greater absolute mositure removal. As for the dehumidification effectiveness, the numerator is the same as the absolute moisture removal. The denominator is the difference between the equivalent humidity content and inlet humidity content of inlet air which are determined by the operating conditions.

Therefore, the explanation for absolute moisture removal also goes for the increment of dehumidification effectiveness. In order to explore the dehumidification enhancement mechanism, some tests, including wetting area and contant angle of plates, were carried out.

3.9 Surface wettability

Fig. 10 presents the wettability of these two different kinds of dehumidiers with the help a high resolution infrared thermal imager made by FLUKE company. The pictures in Fig. 10 were captured under the same operating conditions. As shown in Fig. 10.a, on the surface of ordinary aluminum dehumidifier, the falling film shrank along the flow direction. However, for the anodized one, the shrinking of falling film reduced apparently as shown in Fig. 10.b. By the Microsoft Visio and GetData Graph Digitizer, the wetting area on plate dehumidifer can be measured. It was found that the wetting area increased from 0.143m^2 for ordinary aluminum dehumifier to 0.178m^2 for anodized one with a relative increment of 24.5%. Apart from the wetting area, the contact angles which can represent the wettability of material were also measured on different plates. A standard contact angle goniometer made by Rame-hart instrument Co. with the resolution of 0.1^{o} was employed. The test results are illustrated in Fig. 11. Under the same conditions (solution concentration: 34%, solution temperature: 24^{o}C), the contact angles for ordinary plate and anodized plate are 85.2^{o} and 43.1^{o} respectively. The decrement of contact angle is up to 42.1^{o} which means that the surface energy of ordinargy plate increases significantly after adopting the technology of anodizing. The surface energy is a basic parameter that indicates the surface wettability of material. Generally speaking, material with higher surface energy has better wettability. The thin anodized film on the aluminum plate reduces the surface energy, which leads to the decrement of contact angle and increment of wettting area subsequently.

4 Conclusion

Comparative experiments were carried out to investigate the dehumidification performance of two kinds of single channel dehumidifiers with or without anodizing under various operating conditions. The influence of the main operating conditions was identified. The wetting area and contact angle were also measured under certain conditions to identify the wettability of these two dehumidifiers. Some conclusions are drawn as below:

(1) The newly proposed anodized aluminum dehumidifier showed excellent corrosion resistance performance. Anodized aluminum can be considered as a valuable material for dehumidifier plates in the future.

(2) Compared with the ordinary aluminum dehumidifier, the anodized aluminum dehumidifier shows better wettability. The wetting areas are enlarged from $0.143m^2$ to $0.178m^2$ with a relative increment of 24.5%, and the contact angles decrease from 85.2^o to 43.1^o with a reduction up to 42.1^o under certain conditions.

(3) The operating parameters, such as solution temperature, concentration, and air inlet humidity, directly determine the mass transfer driving force and have obvious effect on the absorption performance. However, other indirect influence parameters, such as solution flow rate and air temperature, show little relationship with the absorption performance. Both the absolute moisture removal and dehumidification effectiveness have a decrement with the increase of air flow rate, but the dehumidification rate will increase due to the co-affect of contact time and mass transfer coefficient.

(4) Under all operating conditions, the anodized aluminum dehumidifier presents a distinct improvement of its dehumidification performance. The enhancement for absolute moisture removal and dehumidification effectiveness can reach up to 50.6% and 36.7% respectively under certain conditions.

To conclude, the newly proposed anodized aluminum can be a good material alternative for falling film dehumidifiers. The results are also valuable for the design of compact dehumidifier made of anodized aluminum and LDCS as well. However, the corrosion resistance performance test in present study only continued for 30 days which is much shorter compared with the service life period of dehumidifiers. Therefore, in our future work, the corrosion resistance performance would be tested by electrochemical methods quantificationally.

Acknowledgement

The work is financially supported by Hong Kong Research Grant Council through General Research Fund (PolyU 152010/15E) and the Hong Kong Polytechnic University through Central Research Grant (PolyU 152110/14E)

References

1. Mei, L. and Y. Dai, *A technical review on use of liquid-desiccant dehumidification for air-conditioning application.* Renewable and Sustainable Energy Reviews, 2008. **12**(3): p. 662-689.
2. Yin, Y., J. Qian, and X. Zhang, *Recent advancements in liquid desiccant dehumidification technology.* Renewable and Sustainable Energy Reviews, 2014. **31**: p. 38-52.
3. Buker, M.S. and S.B. Riffat, *Recent developments in solar assisted liquid desiccant evaporative cooling technology—A review.* Energy and Buildings, 2015. **96**: p. 95-108.
4. Abdel-Salam, A.H. and C.J. Simonson, *State-of-the-art in liquid desiccant air conditioning equipment and systems.* Renewable and Sustainable Energy Reviews, 2016. **58**: p. 1152-1183.
5. Rafique, M.M., P. Gandhidasan, and H.M. Bahaidarah, *Liquid desiccant materials and dehumidifiers–A review.* Renewable and Sustainable Energy Reviews, 2016. **56**: p. 179-195.
6. Abdel-Salam, M.R., R.W. Besant, and C.J. Simonson, *Design and testing of a novel 3-fluid liquid-to-air membrane energy exchanger (3-fluid LAMEE).* International Journal of Heat and Mass Transfer, 2016. **92**: p. 312-329.
7. Fazilati, M.A., A. Sedaghat, and A.A. Alemrajabi, *Natural induced flow due to concentration gradient in a liquid desiccant air dehumidifier.* Applied Thermal Engineering, 2016. **105**: p. 105-117.
8. Fazilati, M.A., A.A. Alemrajabi, and A. Sedaghat, *Liquid desiccant air conditioning system with natural convection.* Applied Thermal Engineering, 2017. **115**: p. 305-314.
9. Luo, Y., et al., *A review of the mathematical models for predicting the heat and mass transfer process in the liquid desiccant dehumidifier.* Renewable and Sustainable Energy Reviews, 2014. **31**: p. 587-599.
10. Khan, A.Y., *Cooling and dehumidification performance analysis of internally-cooled liquid desiccant absorbers.* Applied thermal engineering, 1998. **18**(5): p. 265-281.
11. Ren, C.Q., M. Tu, and H.H. Wang, *An analytical model for heat and mass transfer processes in internally cooled or heated liquid desiccant–air contact units.* International Journal of Heat and Mass Transfer, 2007. **50**(17): p. 3545-3555.
12. Liu, X., et al., *Performance analysis on the internally cooled dehumidifier using liquid desiccant.* Building and Environment, 2009. **44**(2): p. 299-308.
13. Yin, Y., et al., *Model validation and case study on internally cooled/heated dehumidifier/regenerator of liquid desiccant systems.* International journal of thermal sciences, 2009. **48**(8): p. 1664-1671.
14. Jeong, S. and S. Garimella, *Falling-film and droplet mode heat and mass transfer in a horizontal tube LiBr/water absorber.* International Journal of Heat and Mass Transfer, 2002. **45**(7): p. 1445-1458.
15. Yoon, J.-I., et al., *Heat and mass transfer characteristics of a horizontal tube falling film absorber with small diameter tubes.* Heat and Mass Transfer, 2008. **44**(4): p. 437-444.

16. Luo, Y., et al., *Experimental and theoretical research of a fin-tube type internally-cooled liquid desiccant dehumidifier.* Applied Energy, 2014. **133**: p. 127-134.
17. Kim, D. and C.I. Ferreira, *Flow patterns and heat and mass transfer coefficients of low Reynolds number falling film flows on vertical plates: Effects of a wire screen and an additive.* International Journal of Refrigeration, 2009. **32**(1): p. 138-149.
18. Mortazavi, M., et al., *Absorption characteristics of falling film LiBr (lithium bromide) solution over a finned structure.* Energy, 2015. **87**: p. 270-278.
19. Luo, Y., et al., *Experimental study of internally cooled liquid desiccant dehumidification: application in Hong Kong and intensive analysis of influencing factors.* Building and Environment, 2015. **93**: p. 210-220.
20. Luo, Y., et al., *Experimental study of the film thickness in the dehumidifier of a liquid desiccant air conditioning system.* Energy, 2015. **84**: p. 239-246.
21. Yin, Y., et al., *Experimental study on a new internally cooled/heated dehumidifier/regenerator of liquid desiccant systems.* International Journal of Refrigeration, 2008. **31**(5): p. 857-866.
22. Gao, W., et al., *Experimental study on partially internally cooled dehumidification in liquid desiccant air conditioning system.* Energy and Buildings, 2013. **61**: p. 202-209.
23. Zhang, T., et al., *Experimental analysis of an internally-cooled liquid desiccant dehumidifier.* Building and environment, 2013. **63**: p. 1-10.
24. Liu, J., et al., *Experimental analysis of an internally-cooled/heated liquid desiccant dehumidifier/regenerator made of thermally conductive plastic.* Energy and Buildings, 2015. **99**: p. 75-86.
25. Lee, J.H., et al., *Nu and Sh correlations for LiCl solution and moist air in plate type dehumidifier.* International Journal of Heat and Mass Transfer, 2016. **100**: p. 433-444.
26. Conde, M.R., *Properties of aqueous solutions of lithium and calcium chlorides: formulations for use in air conditioning equipment design.* International Journal of Thermal Sciences, 2004. **43**(4): p. 367-382.
27. Handbook, A., *Fundamentals.* American Society of Heating, Refrigerating and Air Conditioning Engineers, Atlanta, 2001. **111**.
28. Coleman, H.W. and W.G. Steele, *Experimentation, validation, and uncertainty analysis for engineers*. 2009: John Wiley & Sons.
29. Kumita, M., et al., *Preparation of calcium chloride-anodized aluminum composite for water vapor sorption.* Applied Thermal Engineering, 2013. **50**(2): p. 1564-1569.

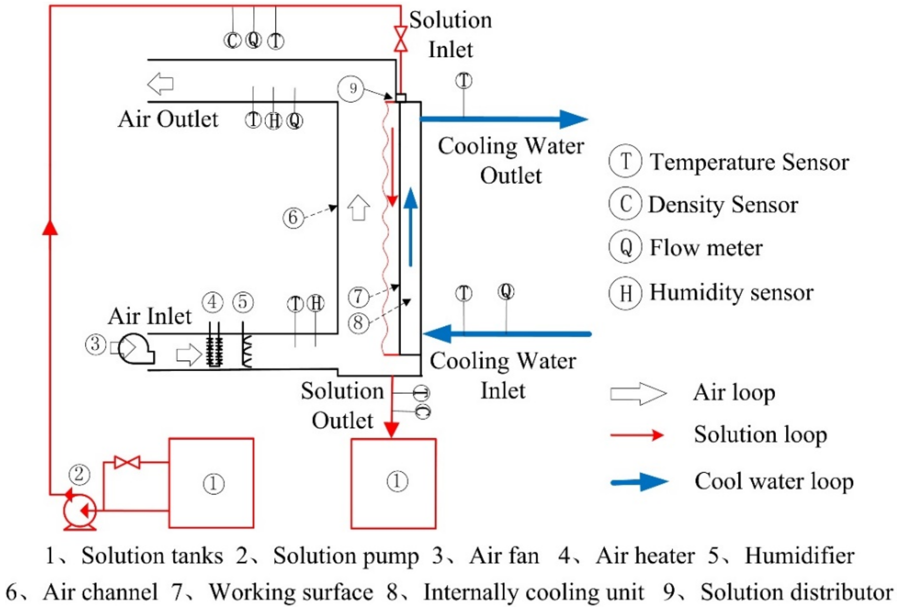

Figure. 1. Schematic diagram of the test rig.

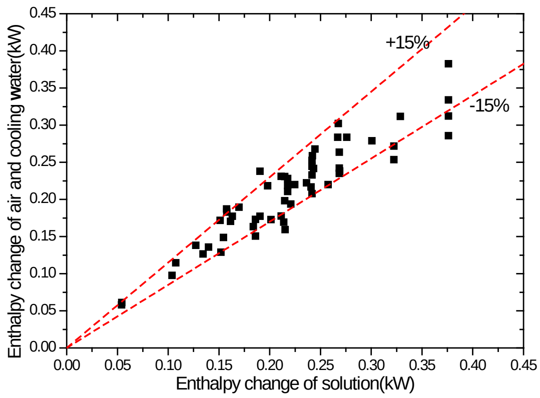

Figure. 2. Energy balance validation of the test rig.

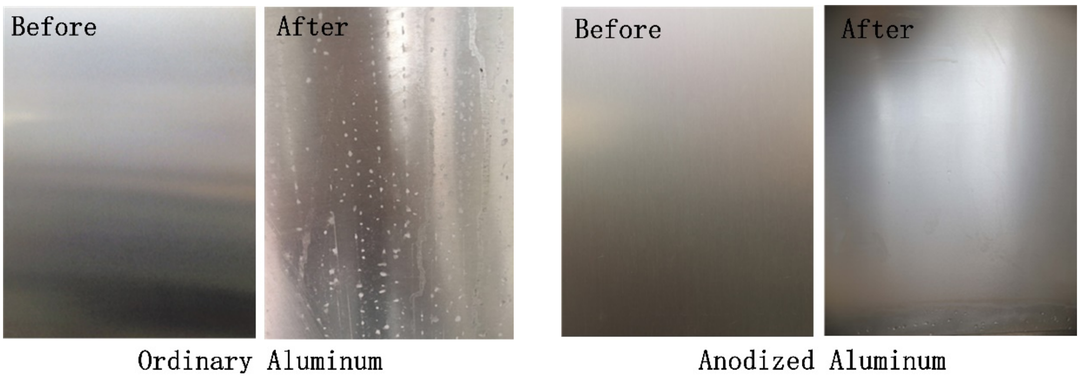

Figure. 3. The results of corrosion resistance ability test:

Left: ordinary aluminum, Right: Anodized aluminum.

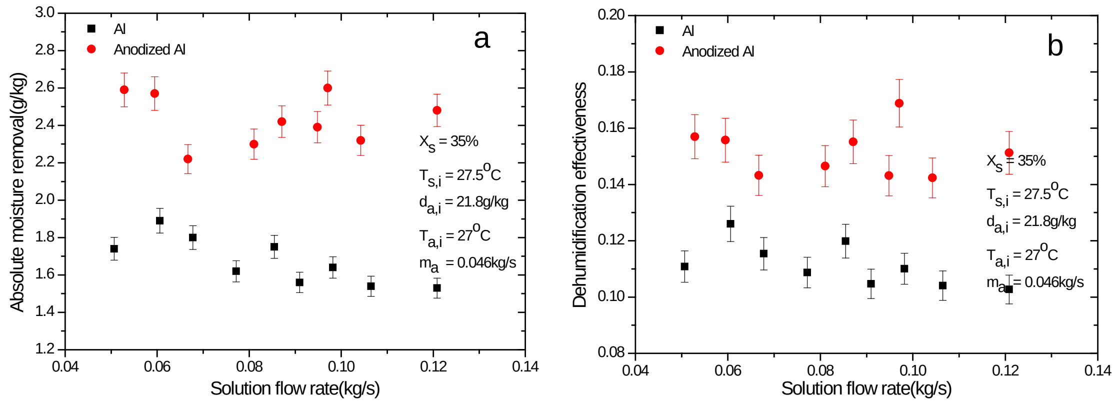

Figure. 4. Influence of solution flow rate on dehumidification performance:

(a) absolute moisture removal, (b) dehumidification effectiveness.

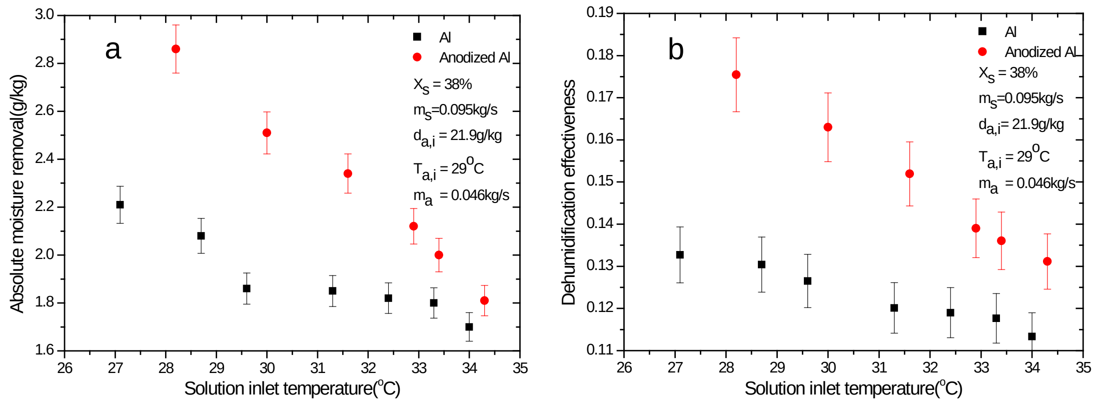

Figure. 5. Influence of solution inlet temperature on dehumidification performance:

(a) absolute moisture removal, (b) dehumidification effectiveness.

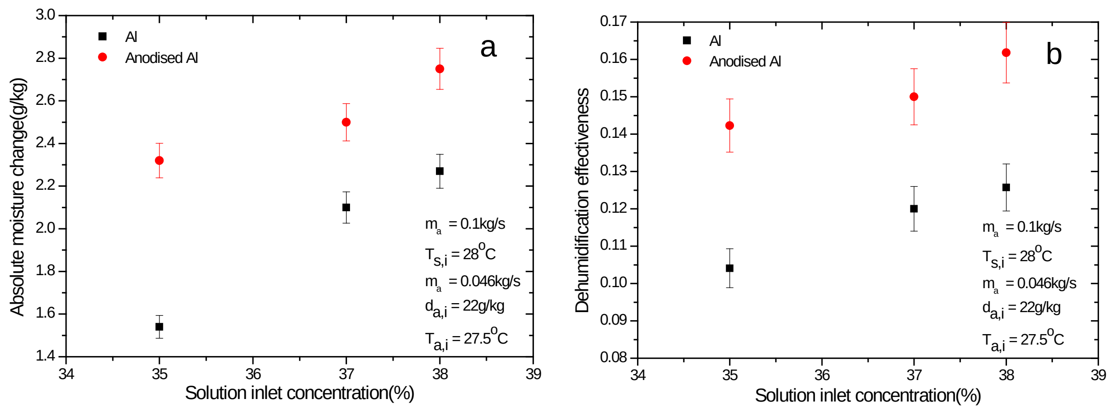

Figure. 6. Influence of solution concentration on dehumidification performance:

(a) absolute moisture removal, (b) dehumidification effectiveness.

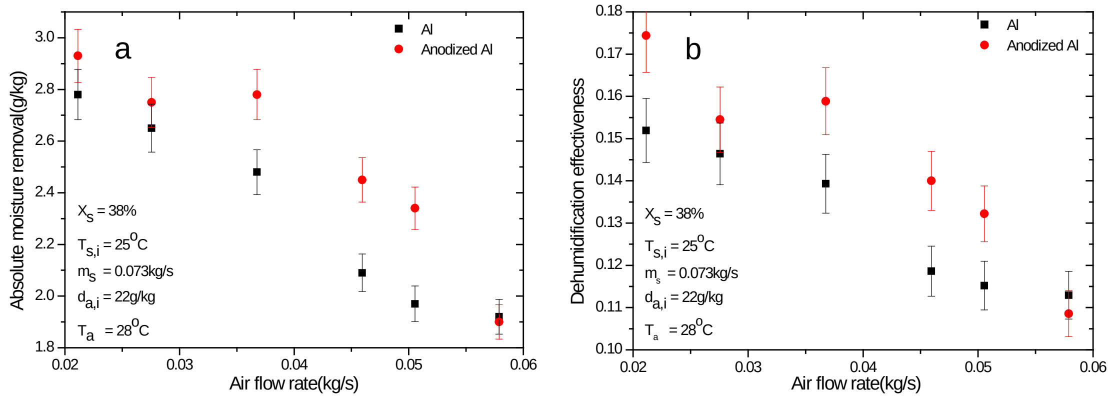

Figure. 7. Influence of air flow rate on dehumidification performance:

(a) absolute moisture removal, (b) dehumidification effectiveness.

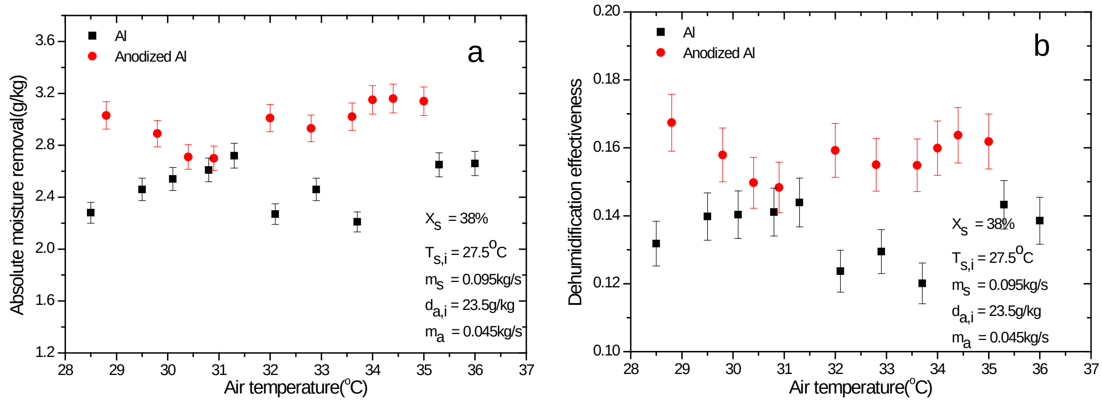

Figure. 8. Influence of air inlet bulb temperature on dehumidification performance:

(a) absolute moisture removal, (b) dehumidification effectiveness.

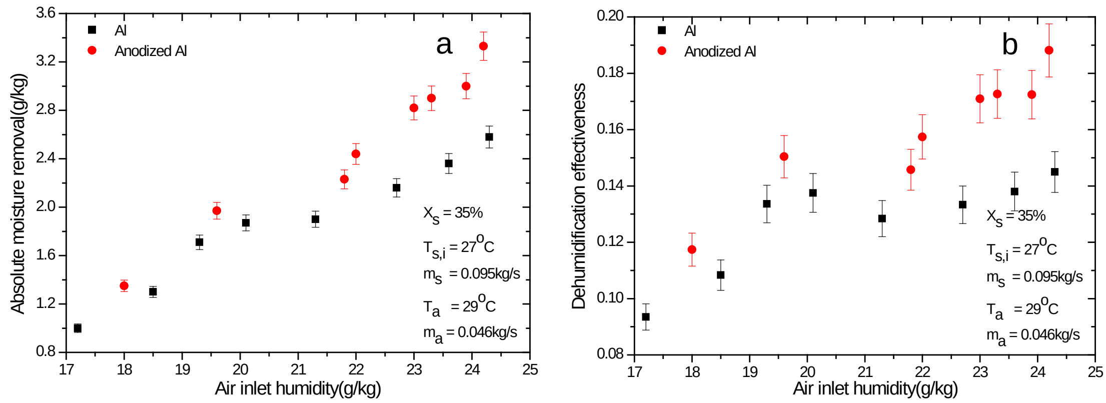

Figure. 9. Influence of air inlet humidity on dehumidification performance:

(a) absolute moisture removal, (b) dehumidification effectiveness.

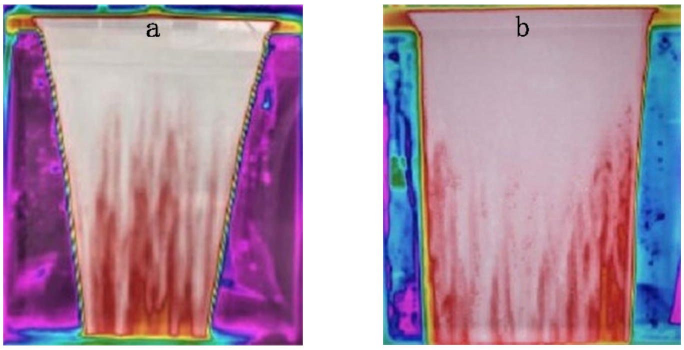

Figure. 10. The contrast of wetting area: (a) ordinary dehumifier, (b) anodized dehumifier.

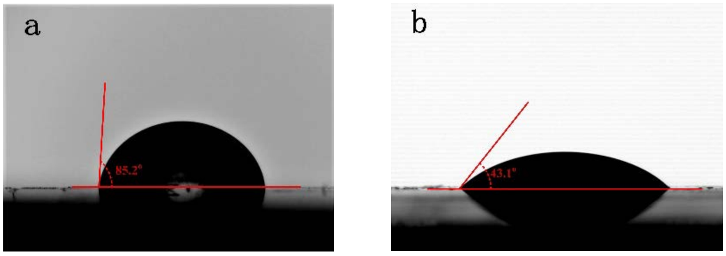

Figure. 11. The contrast between contact angle on: (a) ordinary plate, (b) anodized plate.

Table. 1. Summary of the experimental operating conditions.

Fluid	Parameter	Range
Solution	Concentration (wt%)	35-38
	Mass flow rate (kg/s)	0.05~0.12
	Inlet temperature (°C)	27-34.5
Processing air	Inlet humidity (g/kg)	17-24.5
	Mass flow rate (kg/s)	0.02-0.06
	Inlet temperature (°C)	28-36
Cooling water	Mass flow rate (kg/s)	0.11
	Inlet temperature (°C)	18

Table. 2. Summary of parameters' uncertainties.

Parameter	Uncertainty	Parameter	Uncertainty
All Temperatures/ T	$\pm$ 0.1K	Cooling water flow rate/ G_w	$\pm$ 3%
Solution flow rate/ G_s	$\pm$ 3%	Solution concentration/ X_s	0.2%
Solution density/ ρ_s	$\pm 1kg/m^3$	Air absolute humidity/ d	2.5%
Air flow rate/ G_a	$\pm$ 2.2%	Absolute moisture removal/ Δd	3.5%
Air relative humidity/ φ	$\pm$ 2.5%	Dehumidification effectiveness/ ξ	5.0%